Spherical episodic ejection of material from a young star

J. M. Torrelles*, N. A. Patel†, J. F. Gómez‡, P. T. P. Ho†, L. F. Rodríguez§, G. Anglada‖, G. Garay¶, L. Greenhill†, S. Curiel☆ & J. Cantó☆

** Institut d'Estudis Espacials de Catalunya (IEEC/CSIC) and Instituto de Ciencias del Espacio (CSIC), Gran Capità 2, 08034 Barcelona, Spain*
† Harvard-Smithsonian Center for Astrophysics, 60 Garden Street, Cambridge, Massachusetts 02138, USA
‡ Laboratorio de Astrofísica Espacial y Física Fundamental (INTA), Apdo. Correos 50727, 28080 Madrid, Spain
§ Instituto de Astronomía (UNAM), Apdo. Postal 72-3, 58089 Morelia, México
‖ Instituto de Astrofísica de Andalucía (CSIC), Ap. Correos 3004, 18080 Granada, Spain
¶ Departamento de Astronomía, Universidad de Chile, Casilla 36-D, Santiago, Chile
☆ Instituto de Astronomía (UNAM), Apdo. Postal 70-264, DF 04510, México

The exact processes by which interstellar matter condenses to form young stars are of great interest, in part because they bear on the formation of planets like our own from the material that fails to become part of the star. Theoretical models suggest that ejection of gas during early phases of stellar evolution is a key mechanism for removing excess angular momentum, thereby allowing material to drift inwards towards the star through an accretion disk[1,2]. Such ejections also limit the mass that can be accumulated by the stellar core[1,2]. To date, these ejections have been observed to be bipolar and highly collimated, in agreement with theory. Here we report observations at very high angular resolution of the proper motions of an arc of water-vapour masers near a very young, massive star in Cepheus. We find that the arc of masers can be fitted to a circle with an accuracy of one part in a thousand, and that the structure is expanding. Only a sphere will always produce a circle in projection, so our observations strongly suggest that the perfectly spherical ejection of material from this star took place about 33 years earlier. The spherical symmetry of the ejecta and its episodic nature are very surprising in the light of present theories.

Here we make use of the nature of the 1.35-cm rotational transition of H_2O as a maser (microwave amplification by stimulated emission of radiation), with brightness temperatures exceeding 10^{10} K[3]. The high brightness and the compact nature of masers have proven to be extremely useful in astrophysical very-long-baseline interferometry (VLBI) studies[4]. The very high angular resolution of VLBI allows proper motion studies of masers on the timescales of weeks. This has led to important discoveries, including a new way to measure celestial distances and extremely tight constraints on the mass of supermassive black holes in extragalactic nuclei[5,6].

The star-forming region known as Cepheus A is the second source in the sky ever noted to exhibit the phenomenon of bipolar molecular outflow[7,8]. The driver of the outflow was soon identified as a radio continuum source associated with a high-mass star deeply embedded in high-density molecular gas, which makes it invisible at optical and even at infrared wavelengths. Upon closer study it was revealed to be a biconical radio jet, although its expected associated circumstellar disk was not seen with thermal molecular lines, probably because of their expected faintness[9–13]. However, fortunately, strong H_2O masers are present in this region. Through an experiment on the very large array (VLA) we showed that there is a distribution of masers localized spatially in the form of a flattened disk, centred on the jet, and perpendicular to it[11]. Such a configuration for the disk and the jet is as predicted by theory, because it is the accretion process within the disk which drives the outflow process in the standard model[1].

Using the very long baseline array (VLBA) of the National Radio Astronomy Observatory, we obtained data during three epochs in 1996 in order to study the proper motions of the masers. With an improvement in angular resolution by a factor of 180, we find that most of the unresolved maser features seen on the VLA are now resolved into linear or arclike microstructures (0.4–70 AU).

The detection of the proper motions of these masers depends on a number of considerations: (1) Very accurate relative positions of individual maser features must be achieved, as a proper motion of 10 km s^{-1} at a distance of 725 pc yields an angular displacement of only 3 milliarcseconds (mas) in a year. This is accomplished by phase referencing to a single isolated maser feature. The relative positional accuracy is then a very small fraction of the synthesized beam size, on the order of 50 microarcseconds. (2) The maps at each epoch must be registered relative to each other. Because any individual maser spot can have its own proper motion, referencing to a single maser spot can result in arbitrary offsets in proper motions between epochs. We avoid this problem by using the average position of a number of strong maser spots (spread over a region of about 5 arcsec size) to define a stationary reference position. Although this implicitly assumes that the individual proper motions of the individual maser spots average to zero, we find that this technique in fact works well. In our field of view, we determined proper motions which point in different directions, and which are furthermore systematically perpendicular to the curvatures of the maser structures. This would not be possible if there were a significant component of motion which has been introduced by the use of a nonstationary reference position. (3) Whereas individual parts of a microstructure of masers appear and disappear, the arclike structures can be recognized easily from epoch to epoch. This allowed us to visualize and measure their proper motions as an entire structure.

Here we concentrate on only one particular and most unusual maser feature. In Fig. 1A we show the arcuate structure of masers (hereafter called R5) found south of Cepheus A HW2, at a relatively large distance (500 AU) from the circumstellar disk associated with this young stellar object (YSO). The detected structure, at 100 mas in length, has an angular size similar to that of the VLA beam of the previous observations[11], and is large enough to show up as extended emission in the corresponding VLA maps (Fig. 1B). In contrast, the R5 structure is 200 times the synthesized angular resolution achieved with the VLBA. Such 'large' coherent structures, embedded within a large (5 arcsec) field of view, would have been difficult to map in the early days of VLBI because of the large field of view which must be synthesized, and this has only recently become possible because of the rapid improvements in computing power.

Figure 1C shows that the arc of masers is fitted extremely well by a circle of radius 62 AU. The deviation from the circle is at the level of 0.1% for all three epochs. The proper motions of individual sections of the arc are consistent with uniform expansion perpendicular to the arc at the rate of 9 km s^{-1} with a dynamical timescale of 33 yr (see Fig. 1A). The high degree of symmetry exhibited both by the spatial structure and by the proper motions suggests that we must be seeing the limb-brightened parts of a spherical structure. In particular, the high degree of conformity to a circle makes it unlikely that other structures such as rings or disks or any other geometry might work, because they must lie exactly in the plane of the sky. That the masers are all limb-brightened structures is also consistent with the fact that their line-of-sight local standard of rest (LSR) velocities are nearly the same, meaning that their full three-dimensional proper motions are in fact perpendicular to the line of sight. The lack of masers off the arc suggests that the structure must be an extremely thin shell. That the masers are all located within one quadrant of a circle may suggest that there is another important process that can modify this highly symmetrical outflow. This could be local inhomogeneity or the winds of another source nearby, such as Cepheus A HW2.

We note that this arc structure consists of very small individual

pieces (Fig. 1A), each roughly linear in shape (length sizes of 0.4–1 AU) but being unresolved in the perpendicular direction, and each with a coherent velocity structure which can be described as a single spectral line or feature. The maser emissions in the five subregions indicated in Fig. 1A (labelled a–e) have almost the same radial velocities during the three epochs, with $V_{LSR} = -8.7\,km\,s^{-1}$ (a, c, e), $V_{LSR} = -9.6\,km\,s^{-1}$ (b) and $V_{LSR} = -8.5\,km\,s^{-1}$ (d), (systemic velocity $= -11.7\,km\,s^{-1}$)[11] and line widths $\leq 0.7\,km\,s^{-1}$. The flattened structures and their motions perpendicular to the arc strongly suggest formation and excitation by a shock. The size scale of the individual pieces may be a measure of the thickness of the shell itself. The broken appearance of the masers along the arc is probably due to the nonthermal nature of the masering process as well as instabilities within the thin shell. These data can be seen to support the expectations from theoretical models of shock excitation of water masers[14,15].

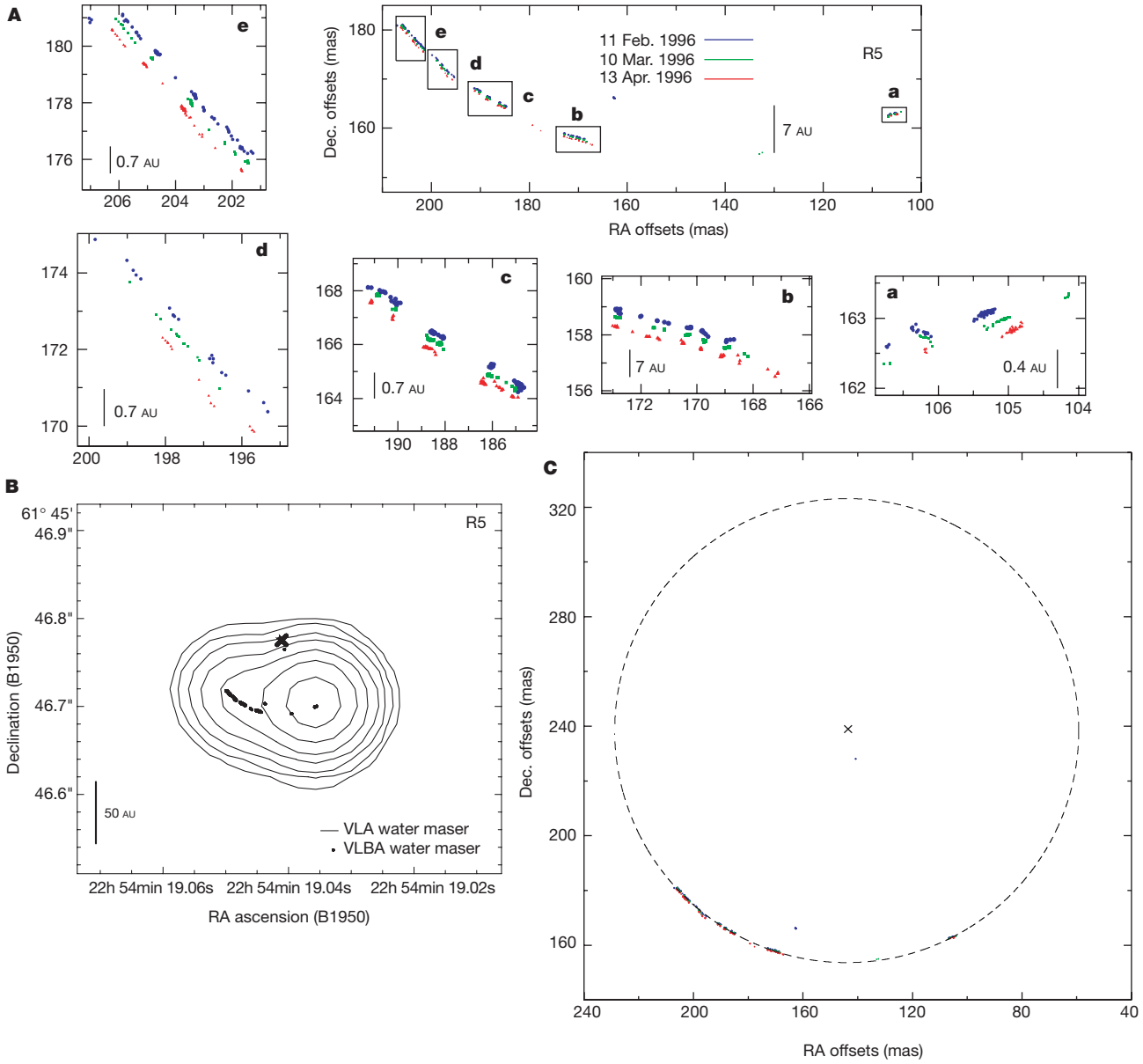

Figure 1 Water maser emission near the young star Cepheus A HW2. The H_2O maser emission (6_{16}–5_{23} line at 22.235 GHz) was observed with the VLBA at an angular resolution of 0.5 mas and a velocity resolution of 0.21 km s^{-1}. We simultaneously mapped for each epoch around 60 fields of 512 × 512 pixels × 245 velocity channels with cell size 0.06 mas. Most of the masers detected with the VLA seven months earlier were detected with the VLBA. We focus on one of the maser features (R5) detected 0.7 arcsec (500 AU) south of Cepheus A HW2, which has been resolved into an arc of 100 mas (72 AU at the distance of 725 pc) in length. **A**, Water maser positions measured with the VLBA. Circles (blue), squares (green), and triangles (red) correspond to the masers detected on 11 February, 10 March and 13 April 1996, respectively. Close-ups of five subregions (labelled **a**–**e**) are also shown. Offset positions are relative to a reference position located at α(J2000) = 22 h 56 min 17.967 s, δ(J2000) = 62° 01′ 48.75″. **B**, Contour map of the water maser emission seen with the VLA on 5 July 1995 towards the region R5 at $V_{LSR} = -8.9\,km\,s^{-1}$. Contour levels are 0.01, 0.02, 0.04, 0.08, 0.16, 0.32, 0.64 × 603 Jy $beam^{-1}$ (VLA beam size is 80 mas)[11]. Dots indicate the positions of the masers constituting the arc microstructure R5 as measured with the VLBA. The cross marks the centre of the circle which is fitted to the arc of masers in the next panel. **C**, The arc structure is fitted by least squares to a circle (including the data of all three epochs). The cross indicates the position of the centre of the circle. Each epoch can be fitted to its own circle to a precision of 0.1%. The radius of the fitted circles is increasing with time, consistent with spherical expansion. There are two maser spots, detected only during the first epoch, which do not fall on the circle. They have radial velocities which disagree with the radial velocity on the circle, suggesting that these are spots which may be lying on the front surface of the spherical shell.

The coherent velocity structure within the arc is seen in Fig. 2, which shows a position–radial velocity (LSR) map of the maser spots in subregion (a) for all three epochs. We note in Fig. 2 that for individual features, for example at distances of 0.3–1.8 mas and $V_{LSR} = -8.5$ to -9.5 km s^{-1}, we can see a clear velocity trend within our synthesized angular resolution of 0.5 mas. This velocity trend persists in all three epochs. Such velocity gradients are probably an indication of a shape or local density gradient so that the shock surface is not completely flat. A curvature in the shock surface, as in a small bow shock structure, results in a spread in projected radial velocity. That the very large velocity wings visible in certain cases seem to be well localized in space, in contrast to the observable velocity gradients in the core of the line, may be a manifestation of the maser amplification process, which favours the line of sight with just the right amplification conditions, and the fact that the shell is very thin. In addition, all of these linear microstructures (a–e) are tangential to the arc curvature, whereas the whole curved structure shows a spatial displacement predominantly perpendicular to the surface of the arc structure (see Fig. 1A).

The observed proper motions and morphology of the arc structure as a whole suggest that it represents a spherical bubble, probably driven by a YSO located at the centre of the circle which fits the arc microstructure. To date, no known continuum source at centimetre wavelengths has been reported at this position[12]. However, since our recognition of this circle of masers, we have examined archival data from the VLA that indicate that a very faint source at 3.6 cm at the level of 0.2 mJy (epoch 1991) may have been present. Further observations with an angular resolution better than tenths of an arcsecond will be important for separating any underlying source from other continuum sources in the region. Submillimetre observations of the dust may also be important if this new centre of star formation activity is deeply embedded. We speculate that the underlying star is probably not a late-type star which typically has a much more irregular shape when observed in water maser emission[16].

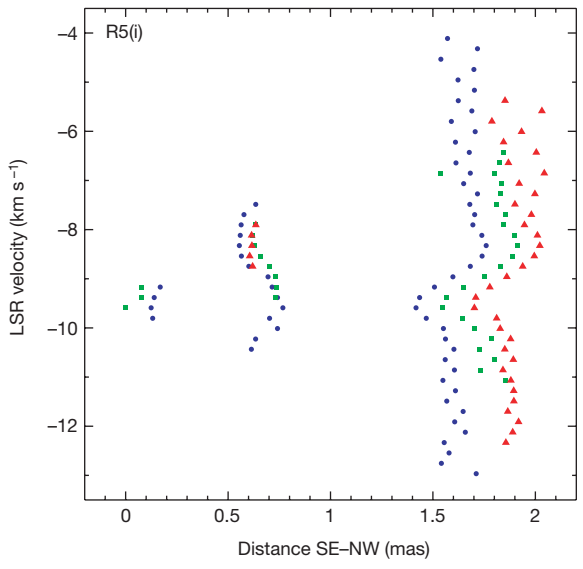

Figure 2 Tracking the velocity structure of the maser spots over two months. This position–velocity (LSR) map of the maser spots in subregion (a) of the arc structure (Fig. 1A) for the three epochs (circles, squares and trianges respectively), has been obtained along an axis with PA $= -68°$, centred on the easternmost maser spot. Velocity structures can be seen to persist in time and are stable in nature. The plot shows that individual maser spots as well as the arc structures can be easily traced from epoch to epoch. The evolution of these velocity structures as well as the circular morphology of the shell of masers will be very interesting problems to study in the future. Given the short dynamical age of 33 yr, we expect that significant changes can be seen in future proper-motion VLBI studies.

The extremely uniform shape and thinness of the R5 arc suggest that the observed material must derive from a single ejection event of short duration. For the same reasons, it is also likely that the masering material is not from local material which is being swept but rather is direct ejecta from the young star itself. Otherwise, local interactions in the sweeping process would not result in such a coherent structure at the 0.1% level. Nevertheless, there are local structural perturbations and large velocity dispersions in the arc structure. If these local differences are present in the initial ejection, again, we would expect that the overall morphology would not be coherent by the time the structure has reached its present size. We speculate that a possible scenario is an initially smoothly expanding shell which is now overtaken by a second episode of ejection. The strongest support for this conjecture may be the very large spread in velocity seen in the line wings in some of the spots which remain localized within the arc structure.

The detection of maser structures organized into arcs and other shapes, both on large (0.1 arcsec) and small (1 mas) scales, have also been reported previously[17–19]. Some of the more recent studies such as the remarkable microstructures in S106IR[20] (bow-shock) and IRAS 21391+5802[21] (loop) also support shock excitation. In particular, the S106IR bow-shock appears to be created by the impact of a very collimated jet with ambient matter. However, all of these maser structures are typically very irregular in shape and kinematics. The uniqueness of our results in R5 lies in the extreme circular symmetry and apparent smoothness of the structure and the ability to trace a very large fraction of the circle. These results are perhaps the best evidence yet for masers tracing a shock front. In addition, the remarkable linear 'building blocks' forming the R5 arc structure suggest that although the structure of the shock front depends on the local conditions, the shock front itself is continuous and organized over a very large solid angle as subtended from the exciting source. Symmetrical structures can be distorted easily by any number of means including ambient density structures or magnetic fields, but an inherently asymmetrical structure cannot easily be made to appear symmetrical. These results suggest that the ejection process in young stellar systems, at least in this case, is highly spherically symmetric, short-lived, and episodic in the beginning. □

Received 29 December 2000; accepted 21 March 2001.

1. Shu, F. H., Adams, F. C. & Lizano, S. Star formation in molecular clouds—Observations and theory. *Annu. Rev. Astron. Astrophys.* **25,** 23–81 (1987).
2. Lizano, S. & Torrelles, J. M. (eds) Circumstellar disks, outflows, and star formation. *Rev. Mex. Astron. Astrofis. Ser. Conf.* **1,** (1995).
3. Cheung, A. C., Rank, D. M., Townes, C. H., Thornton, D. D. & Welch, W. J. Detection of water in interstellar regions by its microwave radiation. *Nature* **221,** 626–628 (1969).
4. Reid, M. J. & Moran, J. M. Masers. *Annu. Rev. Astron. Astrophys.* **19,** 231–276 (1981).
5. Genzel, R., Reid, M. J., Moran, J. M. & Downes, D. Proper motions and distances of H_2O maser sources. I—The outflow in Orion-KL. *Astrophys. J.* **244,** 884–902 (1981).
6. Miyoshi, M. *et al.* Evidence for a black hole from high-rotation velocities in a sub-parsec region of NGC4258. *Nature* **373,** 127–129 (1995).
7. Rodríguez, L. F., Ho, P. T. P. & Moran, J. M. Anisotropic mass outflow in Cepheus A. *Astrophys. J.* **240,** L149–L152 (1980).
8. Ho, P. T. P., Moran, J. M. & Rodríguez, L. F. Mass outflow in star formation regions—Cepheus A. *Astrophys. J.* **262,** 619–635 (1982).
9. Torrelles, J. M., Rodríguez, L. F., Cantó, J. & Ho, P. T. P. A circumstellar molecular gas structure associated with the massive young star Cepheus A-HW 2. *Astrophys. J.* **404,** L75–L78 (1993).
10. Rodríguez, L. F. *et al.* Cepheus A HW2: A powerful thermal radio jet. *Astrophys. J.* **430,** L65–L68 (1994).
11. Torrelles, J. M. *et al.* The thermal radio jet of Cepheus A HW2 and the water maser distribution at 0.08″ scale (60 AU). *Astrophys. J.* **457,** L107–L111 (1996).
12. Torrelles, J. M. *et al.* Systems with H_2O maser and 1.3 centimeter continuum emission in Cepheus A. *Astrophys. J.* **509,** 262–269 (1998).
13. Hughes, V. A. & Wouterloot, J. G. A. The star-forming region in Cepheus A. *Astrophys. J.* **276,** 204–210 (1984).
14. Elitzur, M., Hollenbach, D. J., McKee, C. F. Planar H_2O masers in star-forming regions. *Astrophys. J.* **394,** 221–227 (1992).
15. Kaufmann, M. J. & Neufeld, D. A. Water maser emission from magnetohydrodynamic shock waves. *Astrophys. J.* **456,** 250–263 (1996).
16. Marvel, K. B. The circumstellar environment of evolved stars as revealed by studies of circumstellar water masers. *Publ. Astron. Soc. Pacif.* **109,** 1286–1287 (1997).

17. Gwinn, C. R. Hypersonic acceleration and turbulence of H_2O masers in W49N. *Astrophys. J.* **429,** 241–252 (1994).
18. Leppanen, K., Liljestrom, T. & Diamond, P. Submilliarcsecond linear polarization observations of water masers in W51M. *Astrophys. J.* **507,** 909–918 (1998).
19. Claussen, M. J., Marvel, K. B., Wootten, A. & Wilking, B. A. Distribution and motion of the water masers near IRAS 05413-0104. *Astrophys. J.* **507,** L79–L82 (1998).
20. Furuya, R. S. *et al.* A microjet: a protostar's cry at birth. *Astrophys. J.* **542,** L135–L138 (2000).
21. Patel, N. A. *et al.* Proper motion of water masers associated with IRAS 21391+5802: Bipolar outflow and an AU-scale dusty circumstellar shell. *Astrophys. J.* **538,** 268–274 (2000).

Acknowledgements

NRAO is operated by Associated Universities, Inc., under cooperative agreement with the National Science Foundation. This work was partially supported by MCYT and Programa de Cooperación con Iberoamérica (Spain), and DGAPA and CONACyT (México).

Correspondence and requests for materials should be addressed to P.T.P.H. (e-mail: ho@cfa.harvard.edu).

Observation of the ideal Josephson effect in superfluid ^{4}He

Kalyani Sukhatme*, Yury Mukharsky*†, Talso Chui* & David Pearson*

* *Jet Propulsion Laboratory, California Institute of Technology, Pasadena, California 91109, USA*
† *CEA-DRECAM, Service de Physique de l'État Condensé, Centre d'Études de Saclay, 91191 Gif-sur-Yvette Cedex, France*

Superfluids and superconductors are the only states of condensed matter that can be described by a single wavefunction, with a coherent quantum phase Φ. The mass flow in a superfluid can be described by classical hydrodynamics for small flow velocity, but above a critical velocity, quantized vortices are created and the classical picture breaks down. This can be observed for a superfluid flowing through a microscopic aperture when the mass flow is measured as a function of the phase difference across the aperture; the curve resembles a hysteretic sawtooth where each jump corresponds to the creation of a vortex[1–3]. When the aperture is made small enough, the system can enter the so-called 'ideal' Josephson regime[1,4], where the superfluid mass flow becomes a continuous function of the phase difference. This regime has been detected[1,5,6] in superfluid ^{3}He, but was hitherto believed to be unobservable, owing to fluctuations[7], in ^{4}He. Here we report the observation of the ideal Josephson effect in ^{4}He. We study the flow of ^{4}He through an array of micro-apertures and observe a transition to the ideal Josephson regime as the temperature is increased towards the superfluid transition temperature, T_λ.

In 1962, Josephson[2] predicted that if two superconductors are separated by a thin insulator, then the superposition of the wavefunctions of the bulk superconductors causes the current through the junction to depend sinusoidally on the difference in phase[8], $I = I_c\sin(\phi)$. This equation is known as the d.c. Josephson relation. Here, ϕ is the phase difference $(\Phi_1 - \Phi_2)$ between the two bulk systems. Similar current–phase relationships, $I(\phi)$, are observed in other superconductor/superfluid systems with a separating constriction/insulator (these systems are generally known as 'weak links'). Such systems exhibit a variety of $I(\phi)$ relationships of which non-hysteretic ones are referred to as demonstrating the ideal Josephson effect[4]. In order to observe the ideal Josephson effect, it is necessary for the dimensions of the weak link to be comparable to the minimal length over which the wavefunction can change (coherence length, ξ). The velocity of superflow, v_s, is proportional to the phase difference across the link. This phase difference can be changed by application of a pressure differential, ΔP, according to the a.c. Josephson–Anderson relation[3] $\dot{\phi} = -(m_4/\hbar)(\Delta P/\rho)$ (ρ is the helium density, m_4 is the mass of a Helium atom). As ϕ increases, so does the velocity, until its critical value is reached. When the link dimension is much larger than the coherence length, the critical velocity corresponds to a phase difference greater than 2π. In this regime, the mass current, I, is also proportional to the phase difference, because the current density is given by $\rho_s v_s$, where ρ_s is the density of the superfluid fraction. Thus, the current–phase relationship is linear up to a critical velocity at which one or more 'phase slip' events[5] occur, resulting in a decrease in the phase difference by an integral multiple of 2π. Each 'phase slip' reduces the current by a quantized amount and thus dissipates the kinetic energy of the flow. The system is said to be in the phase-slip regime. As the coherence length is increased (by approaching the superfluid transition, for example) relative to the link size, the critical velocity decreases and corresponds to a smaller phase difference. However, 2π phase slips cannot happen at a phase lower than π, because this would increase the energy. Instead, it becomes energetically favourable to reduce the amplitude of the wavefunction (proportional to ρ_s) within the link[4] as the phase difference approaches π. The $I(\phi)$ becomes non-hysteretic (continuous). Here, the system is in the Josephson regime. By combining the d.c. and a.c. Josephson relations, one obtains $I = I_c\sin(\int -(m_4/\hbar)(\Delta P/\rho)\mathrm{d}t)$. Thus, it is clear that both positive and negative values of the current can result from the application of a positive pressure head. We call this feature (which is very characteristic of the Josephson regime) the 'negative inertia' of the liquid. Another sign of entering the Josephson regime is the disappearance of the dissipation associated with the phase slips. Our experiments provide the first direct evidence of these two facts in ^{4}He.

Electron-beam lithography techniques permit us to make structures with dimensions of the order of 0.1 μm. This is comparable to

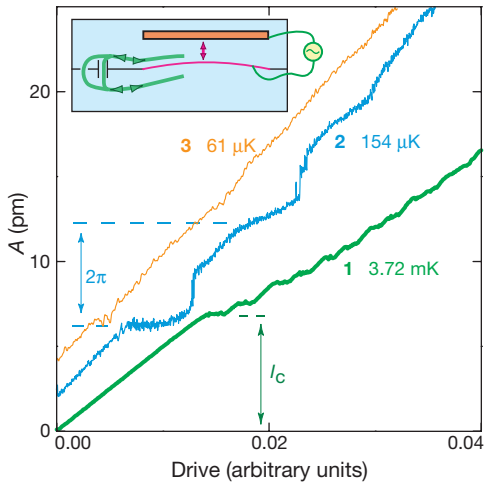

Figure 1 Staircase patterns (amplitude versus drive). $T_\lambda - T$ is 3.72 mK (**1**); 154 μK (**2**); 61 μK (**3**). The data for curve **1** has been divided by 20 in *x* and by 10 in *y*. The plots are shifted 2 pm for clarity. The height of the first step corresponds to the critical current I_c, as marked. Each subsequent step corresponds to an additional phase difference of 2π, as marked. The insert shows the schematics of the cell: it consists of a two-chamber resonator connected by a flow path. One of the walls between the two chambers is a flexible diaphragm made of thin metallized kapton. The diaphragm and the adjacent wall of the volume form a capacitor, which is used to apply an a.c. pressure drive to the resonator. The drive, in concert with the pressure difference exerted across the flow path by the diaphragm, generates a helium flow. Diaphragm motion is measured with a SQUID-based position sensor with a resolution of about 2×10^{-13} m Hz$^{-1/2}$. The calibration of this position sensor is difficult and thus the magnitudes of displacements or currents cited here should be taken as estimates only. The temperature of the cell is controlled using high-resolution thermometers[15] with nano-Kelvin temperature stability.